Glucocorticoid receptor antagonist CORT113176 attenuates motor and neuropathological symptoms of Huntington's disease in R6/2 mice

Gentenaar, M.; Meulmeester, F.L.; Burg, X.R. van der; Hoekstra, A.T.; Hunt, H.; Kroon, J.; ... ; Meijer, O.C.

Experimental Neurology 374 (2024) 114675

Contents lists available at ScienceDirect

Experimental Neurology

journal homepage: www.elsevier.com/locate/yexnr

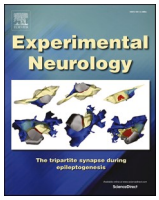

Research paper

Glucocorticoid receptor antagonist CORT113176 attenuates motor and neuropathological symptoms of Huntington's disease in R6/2 mice

Max Gentenaar [a,*], Fleur L. Meulmeester [a], Ximaine R. van der Burg [a], Anna T. Hoekstra [a,b], Hazel Hunt [c], Jan Kroon [a,c], Willeke M.C. van Roon-Mom [d], Onno C. Meijer [a]

[a] Department of Medicine, Division of Endocrinology, Leiden University Medical Center, Leiden, the Netherlands
[b] Center for Proteomics and Metabolomics, Leiden University Medical Center, Leiden, the Netherlands
[c] Corcept Therapeutics, Menlo Park, CA, USA
[d] Department of Human Genetics, Leiden University Medical Center, Leiden, the Netherlands

ARTICLE INFO

Keywords:
Neurodegeneration
Corticosterone
HPA-axis
Astrocytosis
Microgliosis
Sexual dimorphism

ABSTRACT

Huntington's Disease (HD) is a progressive neurodegenerative disease caused by a mutation in the huntingtin gene. The mutation leads to a toxic gain of function of the mutant huntingtin (mHtt) protein resulting in cellular malfunction, aberrant huntingtin aggregation and eventually neuronal cell death. Patients with HD show impaired motor functions and cognitive decline. Elevated levels of glucocorticoids have been found in HD patients and in HD mouse models, and there is a positive correlation between increased glucocorticoid levels and the progression of HD. Therefore, antagonism of the glucocorticoid receptor (GR) may be an interesting strategy for the treatment of HD. In this study, we evaluated the efficacy of the selective GR antagonist CORT113176 in the commonly used R6/2 mouse model. In male mice, CORT113176 treatment significantly delayed the loss of grip strength, the development of hindlimb clasping, gait abnormalities, and the occurrence of epileptic seizures. CORT113176 treatment delayed loss of DARPP-32 immunoreactivity in the dorsolateral striatum. It also restored HD-related parameters including astrocyte markers in both the dorsolateral striatum and the hippocampus, and microglia markers in the hippocampus. This suggests that CORT113176 has both cell-type and brain region-specific effects. CORT113176 delayed the formation of mHtt aggregates in the striatum and the hippocampus. In female mice, we did not observe major effects of CORT113176 treatment on HD-related symptoms, with the exception of the anti-epileptic effects. We conclude that CORT113176 effectively delays several key symptoms related to the HD phenotype in male R6/2 mice and believe that GR antagonism may be a possible treatment option.

1. Introduction

Huntington's Disease (HD) is a progressive neurodegenerative disease caused by an expansion in the number of CAG repeats (35+) in the huntingtin (*HTT*) gene. The mutation leads to an expanded stretch of glutamine amino acids in the N-terminus of the huntingtin (htt) protein resulting in a toxic gain of function of the mutant huntingtin (mHtt) protein. The underlying mechanisms of HD pathology are extensive, and include deregulation of many cellular processes such as the ubiquitin-proteasome system, the autophagy system and aberrant protein-protein interactions (Bates et al., 2015). The mHtt aggregates are the neuropathological hallmarks of the disease. Patients with HD suffer from cognitive decline, motor deficits, chorea movements, psychiatric disorders, muscle wasting and metabolic dysfunctions (Vonsattel and DiFiglia, 1998; Kirkwood et al., 2001).

Multiple studies have shown a positive correlation between increased glucocorticoid levels and the progression of HD in patients (Aziz et al., 2009; van Duijn et al., 2010; Bartlett et al., 2016). High levels of endogenous glucocorticoids have been linked to several HD-related symptoms including neurodegeneration, cognitive decline, muscular atrophy and metabolic dysfunctions (Vyas et al., 2016; Schakman et al., 2013; Vegiopoulos and Herzig, 2007). These symptoms are recapitulated in the R6/2 mouse strain, the most commonly used HD model, that exhibits mHtt aggregates, various motor symptoms and

* Corresponding author at: Department of Medicine, Division of Endocrinology, Leiden University Medical Center (LUMC), Albinusdreef 2, 2333ZA, Leiden, the Netherlands.
E-mail address: m.gentenaar@lumc.nl (M. Gentenaar).

https://doi.org/10.1016/j.expneurol.2024.114675
Received 12 May 2023; Received in revised form 17 November 2023; Accepted 2 January 2024
Available online 10 January 2024

increased levels of corticosterone (Bjorkqvist et al., 2006; Dufour and McBride, 2016; Morton et al., 2000). These symptoms are aggravated in R6/2 mice after exposure to acute or chronic stress, and are therefore likely affected by elevated levels of glucocorticoids (Mo et al., 2013; Mo et al., 2014). Reducing the corticosterone levels in the R6/2 mice by adrenalectomy delays neurological symptoms such as reduction of brain mass and the formation of mHtt aggregates (Dufour and McBride, 2019). These effects are likely mediated through the glucocorticoid receptor (GR). Taken together, there is a clear contribution of glucocorticoid signaling to the pathology of HD in the R6/2 model, and GR antagonism may therefore be an interesting treatment strategy for HD.

The most commonly used GR antagonist, mifepristone (RU486), also has affinity for the progesterone receptor (PR) and the androgen receptor (AR) and this lack of selectivity can cause side effects (Gaillard et al., 1984). Mifepristone showed striking effects in animal models for other neurodegenerative diseases, but the lack of selectivity precludes formal conclusions on GR involvement in such settings (Baglietto-Vargas et al., 2013; Lesuis et al., 2018). The GR antagonist CORT113176 (K_i = 0.16 nM, Fig. 1) lacks cross-reactivity with other steroid receptors and it has already been proven to be effective in models for Alzheimer's disease and amyotrophic lateral sclerosis (ALS) (Hunt et al., 2015; Pineau et al., 2016; Meyer et al., 2018; Meyer et al., 2020).

In this study, we evaluated the potential of CORT113176 to attenuate the symptoms of HD in R6/2 mice. We showed that treatment with CORT113176 delayed several motor symptoms in male mice, but less so in female HD mice. Region-specific changes on glial cells in HD mice were normalized by CORT113176 treatment. Finally, treatment with CORT113176 reduced the formation of hippocampal CA1 and striatal mHtt aggregates.

2. Material & methods

2.1. Animals

All mouse experiments were reviewed by the animal welfare body of Leiden University Medical Center (IvD Leiden) and executed under a license granted by the Central Authority for Scientific Procedures on Animals (CCD) under the license number AVD1160020198404, in accordance with the Dutch Act on Animal Experimentation and EU Directive 2010/63/EU.

HD and wild-type (WT) R6/2 mice were purchased from JAX (The Jackson Laboratory, ME, USA) and arrived in the animal facility at 4-weeks of age. The mice were housed under normal conditions (room temperature, 12 h light/dark cycle) with food and water *ab libitum*. The mice were housed 3–4 per cage, separated by sex, but different genotypes were housed together to improve the survival of the HD mice (Story et al., 2021). Genotyping on tail samples that were collected post-mortem was performed by Laragen (CA, USA) to confirm that all HD mice had between 120 and 130 CAG repeats.

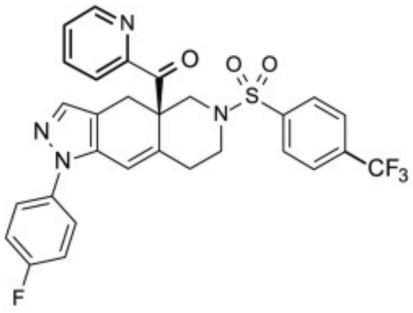

Fig. 1. Chemical structure of CORT113176 or [(4aR)-1-(4-fluorophenyl)-1,4,5,6,7,8-hexahydro-6[[4-trifluoromethyl)phenyl]sulfonyl[-4aH-pyrazolo [3,4-*g*]isoquinolin-4a-yl]-2-pyridinyl]-(R) (Hunt et al., 2015).

2.2. Animal studies: experimental procedures

From 6 weeks of age onwards, mice received a daily *s.c.* injection either with 30 mg/kg of CORT113176 (Corcept Therapeutics, CA, USA) or vehicle (Veh; castor oil in experiment 1 or sesame oil in experiment 2) for five consecutive weeks. In experiment 1, male and female mice were assigned into one of the following groups: 1: WT + Veh ($n = 5$ per sex), 2: WT + CORT113176 (n = 5 per sex), 3: HD + Veh (n = 5 per sex) or 4: HD + CORT113176 (n = 5 per sex). In the final analysis there was an unequal group distribution for the male mice due to a mislabeled genotype and a mouse reaching an earlier endpoint resulting in $n = 6$ in the WT + Veh group and $n = 3$ in the HD + Veh group. In experiment 2, male mice were assigned into the following groups: 1: WT + Veh ($n = 10$), 2: HD + Veh (n = 10) and 3: HD + CORT113176 (n = 10, ultimately $n = 8$ due to a non-responder that met outlier criteria and a mouse reaching an earlier timepoint). Bodyweight was measured weekly and motor tests were performed at 1 PM to monitor the disease progression (as described below). On day 19 and day 34, blood samples were collected via a nick in the tail vein in the morning to evaluate corticosterone levels. On day 34, the animals were sacrificed using CO_2 inhalation, blood was collected via cardiac puncture and the animals were perfused with cold PBS. Afterwards, several tissues of interest were harvested and snap-frozen for further analysis. Half a hemisphere was collected and stored for 24 h at 4% PFA for IHC (further described below).

2.3. Motor function studies

2.3.1. Grip strength

Grip strength measurements were performed weekly to quantify muscle strength. For this procedure, mice were lifted by their tail in front of a metal bar that was attached to a Chatillon Grip Force Meter (Columbus Instruments, OH, USA) and mice were allowed to grasp the grid tightly with both forepaws. The mouse was then gently pulled away until grip was lost, and the force that was required to do this was monitored. This test was repeated 15 times with short resting periods between every 5 measurements (Aartsma-Rus and van Putten, 2014). The average of the three highest scores were used for the analysis.

2.3.2. Clasping test

The clasping test was performed weekly to assess the degradation of the cortico-striatal pathway, the primary input circuity of the basal ganglia that controls many processes including voluntary movement and motor coordination (Haber, 2016). For this procedure, the mice were lifted by their tail to a height of approximately 50 cm for no longer than 10 s. During this procedure, the hindlimbs were observed and a score was given based on their position in relation to the abdomen ranging from 0 to 3 (Guyenet et al., 2010). This was repeated three times and the average of the scores was used for the analysis.

2.3.3. Gait analysis

Gait was measured to examine differences in locomotion using the CatWalk-XT (Noldus Information Technology, Wageningen, The Netherlands) on day 15 and day 29. In this set-up the animals crossed a glass plate through a closed-off pathway and paw placement was recorded. Two days prior to the measurements, the animals were habituated to the environmental set-up for 5 min. During the measurement, the mice completed three successful runs which were defined as an uninterrupted walk across the pathway within 7 s that included at least 10 steps. The runs were recorded and analysed using the CatWalk-XT software (Noldus Information Technology, version 10.6). Within the software the gain was set at 13.6 and the green threshold at 0.10. Runs with an average run speed between 10 and 40 cm/s and a maximum variation of 25% were included in the final analysis.

2.3.4. Epileptic Seizures

several instances of (spontaneous) seizures were observed in the HD

mice throughout the study. Every case was documented and scored using the Racine scale (Van Erum et al., 2019).

2.4. Immunohistochemistry

Brains were isolated and the left hemisphere was fixated in 4% PFA (Sigma-Aldrich, 8,187,085,000) for 24 h. Afterwards the brains were transferred to a 30% sucrose solution in PBS for 24–48 h and stored at −80 °C until further processing. Cryosections of 10 μM were collected (CryoStar NX70) on slides (Avantor, VWR® Microscope Slides, 631–1166) and stored at −20 °C until staining. Striatal cryosections were collected from bregma 0.98 mm - 0.74 mm and hippocampal cryosections from bregma −1.58 mm to −1.94 mm. The slides were incubated for 25 min with 0,1% Triton X-100 (Sigma-Aldrich) in PBS, washed with 0.1% PBS/Tween (Tween®20, Sigma-Aldrich). The background signal was blocked with 5% BSA in PBS for 30 min before incubation with the primary antibody DARPP32 (1:500, abcam, EP720Y, ab40801), GFAP (1500, Agilent DAKO, Z0334), Iba1 (1500, Fujifilm Wako, 019–19,741) or mHtt (1500, abcam, EPR5526, ab209668) in 1% BSA in PBS overnight at 4 °C. The following day slides were washed with 0.1% PBS/Tween before incubation with the secondary antibody goat anti-rabbit Alexa Fluor 488 (1250, Invitrogen, A-110088) for 30 min. After a final wash with 0.1% PBS/Tween, ProLong gold with DAPI (Invitrogen, P36931) was added with a coverslip (Thermo-Fisher, Menzel-Gläser, 0980) and the slides were dried at room temperature. The slides stained for DARPP32, GFAP and Iba1 were scanned with the Axio Slide Scanner (Zeiss, Axio Slide Scan.Z1) and the mHtt slides were imaged using the confocal microscope (Leica, White Light Laser Confocal Microscope TCS SP8 X). All obtained images were analysed using ImageJ (version 1.52p). The mean intensity of DARPP32, GFAP and Iba1 immunofluorescence was measured in the dorsolateral striatum and hippocampus . The total number of aggregates in a specific region of interest (ROI), the total area in the ROI and the average size of the aggregates were measured. A total of 3 sections per mouse were analysed and the average was used for statistical analysis for all measured parameters.

2.5. Corticosterone

Blood samples were diluted 25× to measure corticosterone levels by using the Corticosterone High Sensitivity EIA ELISA kit (Immunodiagnostic Systems, #AC-15F1) following the protocol provided by the manufacturer.

2.6. Gene expression

Frozen tissues were homogenized in Lysing Matrix D Minibead tubes (MP Biomedicals, #116913500) using TriPure isolation reagent (Roche, #11667165001) and total RNA was isolated following the protocol provided by the manufacturer. cDNA was synthesized using M-MLV reverse transcriptase (Promega, #M1705). Real-time quantitative PCR was performed using IQ SYBR-Green Supermix (Bio-Rad, #170–8885) and the Bio-Rad CFX96 system.

Statistical analyses.

All statistical analyses were performed using GraphPad Prism Software version 9.3.1. All data are presented as mean + S.E.M. Data collected over several weeks from experiment 1 were analysed by three-way ANOVA or mixed-effect model if data points were missing. Data collected over time in experiment 2 were analysed by mixed-effects model with repeated measures. Individual time points were analysed by two-way or one-way ANOVA. Epileptic seizures were analysed by Kaplan-Meier and log-rank test by using the first observed occurrence for each mouse. All other data were analysed by either two-way or one-way ANOVA as appropriate and Tukey's multiple comparison was used to analyses differences between groups.

3. Results

3.1. Experiment 1

We present the data of male and female mice separately, given the substantial differences between the sexes in the response to CORT113176 treatment and HPA-axis markers. We provide all main terms from the ANOVA analyses in supplementary tables as indicated.

3.1.1. CORT113176 treatment partially rescues muscle strength in male, but not in female HD mice

Forelimb grip strength was measured to assess the effect of CORT113176 on muscle function. We observed a significant genotype effect over time in both male and female mice (Supplementary 1.A, $p < 0.0001$, $F(5,77) = 6.303$ and Supplementary 1.B, $p < 0.0001$, $F(5,80) = 15.00$). Muscle strength in male WT mice remained relatively stable over the course of five weeks (Fig. 2.A). In contrast, vehicle-treated male HD mice showed a steady decline in grip strength over time, starting from week 2. CORT113176 treatment attenuated this decrease of muscle function in male HD mice, although this did not reach statistical significance.

In female mice, both vehicle- and CORT113176-treated WT groups showed a slight increase in grip strength after five weeks (Fig. 2.B). Both vehicle- and CORT113176-treated female HD groups displayed a decline in grip strength over time. A significant difference was observed between WT and HD female mice from week 3 onwards, but no effect of CORT113176 treatment was observed.

3.1.2. CORT113176 treatment delays clasping score in male, but not in female HD mice

The clasping test was performed as a measure to evaluate the effect of CORT113176 treatment on the functional decline of the cortico-striatal pathway, an important pathway for voluntary movement and motor coordination. A high clasping score indicates loss of voluntary motor coordination and therefore a more progressed HD phenotype. None of the WT mice showed clasping behaviour. We observed a significant genotype effect over time for both sexes (Supplementary table 1.C, $p < 0.0001$, $F(5, 77) = 15.18$ and 1.D, $p < 0.0001$, $F(5,80) = 16.27$).

In male mice, there was a significant interaction effect between HD and CORT113176 (Supplementary 2.C, $p = 0.0018$, $F(1,16) = 13.98$). Vehicle-treated male HD mice showed a significant increase in clasping score starting from week 1 as compared to the WT mice (Fig. 2.C), and CORT113176 treatment significantly reduced clasping score in HD mice as compared to vehicle-treated HD mice.

In female mice, vehicle-treated HD mice showed significant increased clasping over time compared to the WT mice (Fig. 2.D). There was a significant interaction for genotype, CORT113176 treatment and time suggesting that at later timepoints the treatment attenuated the clasping score (Supplementary 1.D, $p = 0.0421$, $F(5,80) = 2.248$).

3.1.3. CORT113176 has no effect on loss or gain of bodyweight

Weekly body weight measurements showed a significant genotype effect over time in both male and female mice (Supplementary 1.E, $p < 0.0001$, $F(6,93) = 10.57$ and 1.F, $p < 0.0018$, $F(6,96) = 3.838$) Both vehicle- and CORT113176-treated male HD mice gained less weight compared to WT mice and had a lower bodyweight at the end of the week 5 (Fig. 2.E). In contrast, vehicle- and CORT113176-treated female HD groups gained more weight compared to the WT (Fig. 2.F).

3.1.4. CORT113176 treatment prevents epileptic seizures in both sexes

Epileptic seizures are a known symptom in Juvenile HD (JHD), a form of HD that affects children and teenagers and this feature is recapitulated in the R6/2 mouse model (Thakor et al., 2021). Total observed epileptic seizures during experimental procedures were documented, which were of tonic-clonic nature according to the Racine scale (Van Erum et al., 2019). Epileptic seizures occurred most frequently in the

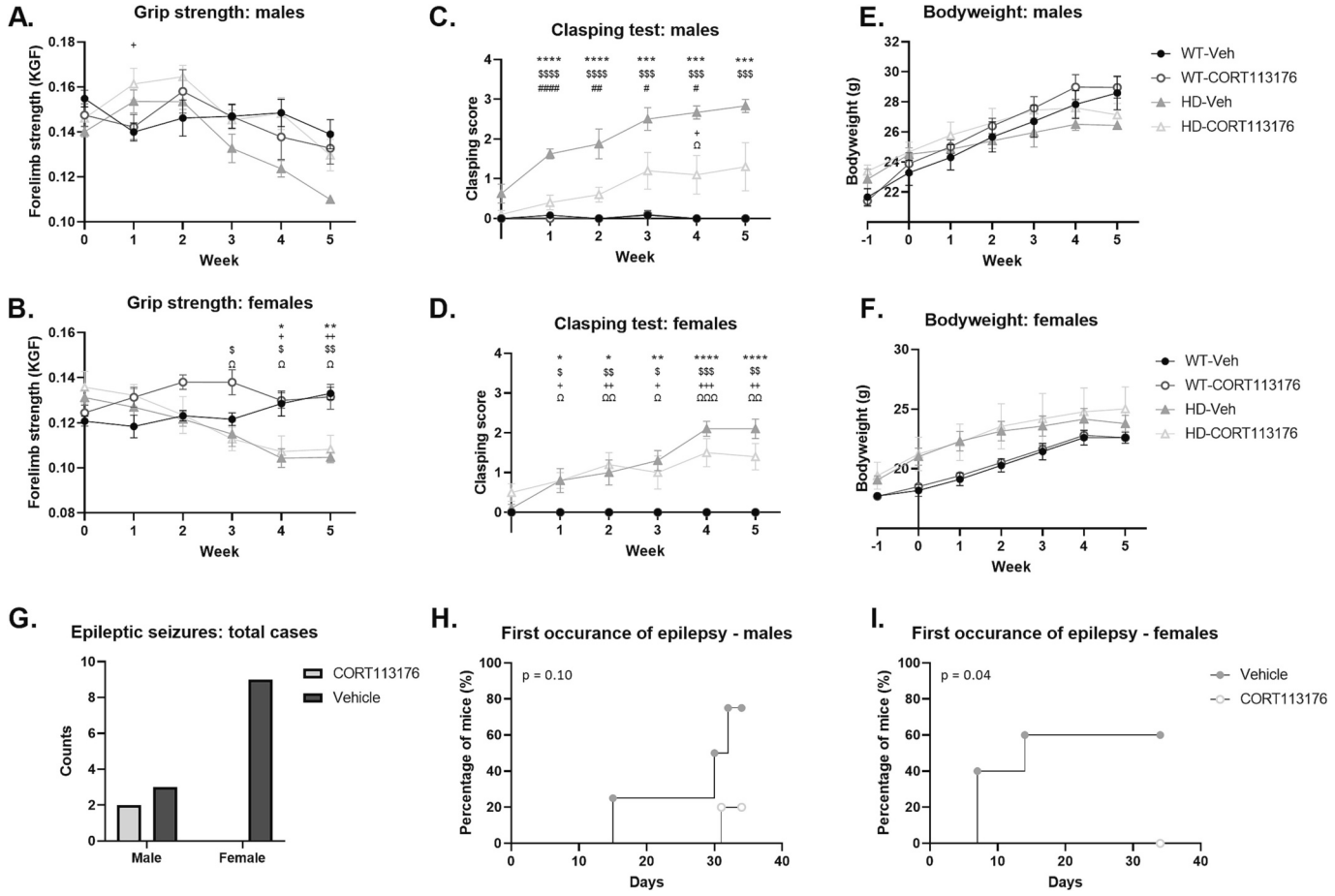

Fig. 2. Effects of the HD genotype and CORT113176 treatment on functional parameters in male and female R6/2 mice. (A) Forelimb grip strength measured over time of males and (B) of females. (C) Hindlimb clasping score measured over time of males and (D) of females. (E) Body weight gain measured over time of males and (F) of females. (G) Total number of epileptic seizures of both males and females. (H) Kaplan-Meier analysis for first occurrences of epilepsy in males and (I) and females. (A-F) Data presented as mean + S.E.M. and analysed by three-way ANOVA or mixed effect model. Individual timepoints were analysed by two-way ANOVA with Tukey's multiple comparison represented as $*p < 0.05$, $**p < 0.01$, $***p < 0.001$,$****p < 0.0001$ (* = WT-Veh vs HD-Veh, $ = WT-CORT113176 vs HD-Veh, # = HD-CORT113176 vs HD-Veh, + = WT-Veh vs HD-CORT113176 and Ω = WT-CORT113176 vs HD-CORT1113176). Missing values are due to significant outliers or technical errors.

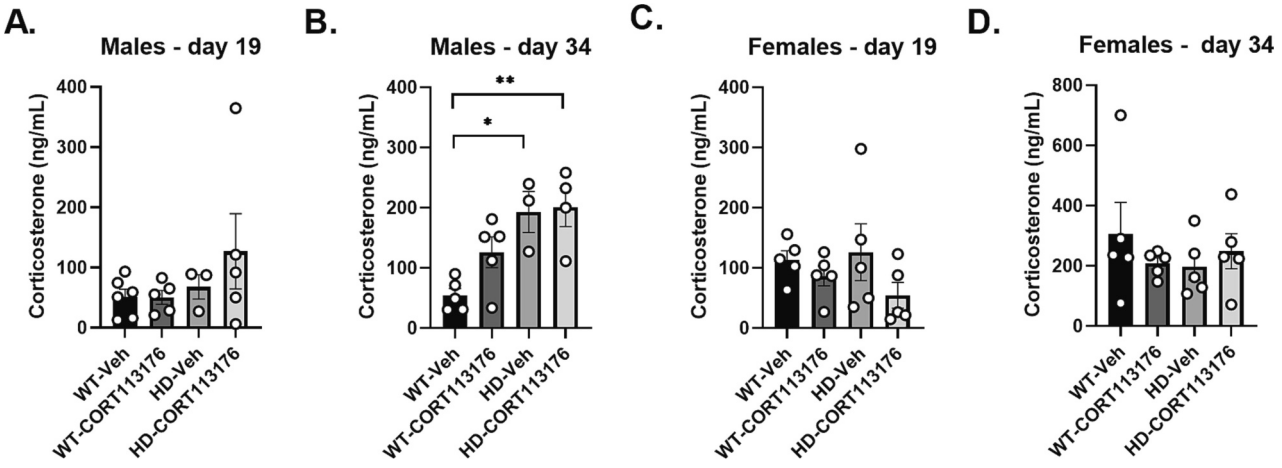

Fig. 3. Corticosterone levels of male and female R6/2 mice at different timepoints. (A) Corticosterone levels of males at 1 PM on day 19. (B) Corticosterone levels of males at 1 PM on day 34. (C) Corticosterone levels of females at 1 PM on day 19. (D) Corticosterone levels of females at 1 PM on day 34. Data presented as mean + S.E.M. and analysed by two-way ANOVA with Tukey's multiple comparison represented as * $p < 0.05$, ** $p < 0.01$, *** $p < 0.001$,**** $p < 0.0001$. Missing values are due to significant outliers or technical errors.

vehicle-treated female HD mice, while none were observed in the CORT113176-treated female HD mice (Fig. 2.G). Overall, epileptic seizures were less common in the male HD mice, although these also occurred slightly more frequently in the vehicle-treated HD mice as compared to the CORT113176-treated HD male mice (Fig. 2.G). The epileptic seizures in the CORT113176-treated HD mice occurred mostly near the end of the five weeks (day 32) while the cases of the vehicle-treated HD animals occurred throughout the whole 5-week study (Fig. 2.H, $p = 0.10$ and 2.I, $p = 0.04$).

3.1.5. Increased levels of corticosterone in male, but not in female R6/2 mice

Blood samples were collected in the morning, during the trough of the circadian rhythm of mice, to measure corticosterone levels. On day 19, there was no difference in corticosterone in either of the male groups (Fig. 3.A). On day 34, a significant increase of corticosterone levels was observed in both vehicle- and CORT113176-treated HD male mice compared to the vehicle-treated WT mice (Fig. 3.B, HD: $p = 0.0012$, F (1,13) = 17.19) and this increase was unaffected by CORT113176 treatment. In the female animals, we did not observe differences in corticosterone levels between groups on day 19 nor day 34 (Fig. 3.C and 3.D).

3.1.6. CORT113176 did not prevent loss of DARPP-32 expression and has region-specific effects on glial cells

Several biomarkers relevant to the HD phenotype were assessed using immunohistochemical analysis of the brain. Neurodegeneration in the striatum, the most prominently affected brain region in HD, was evaluated by dopamine- and cAMP-regulated phosphoprotein (DARPP32) staining, a marker for striatal medium spiny neurons

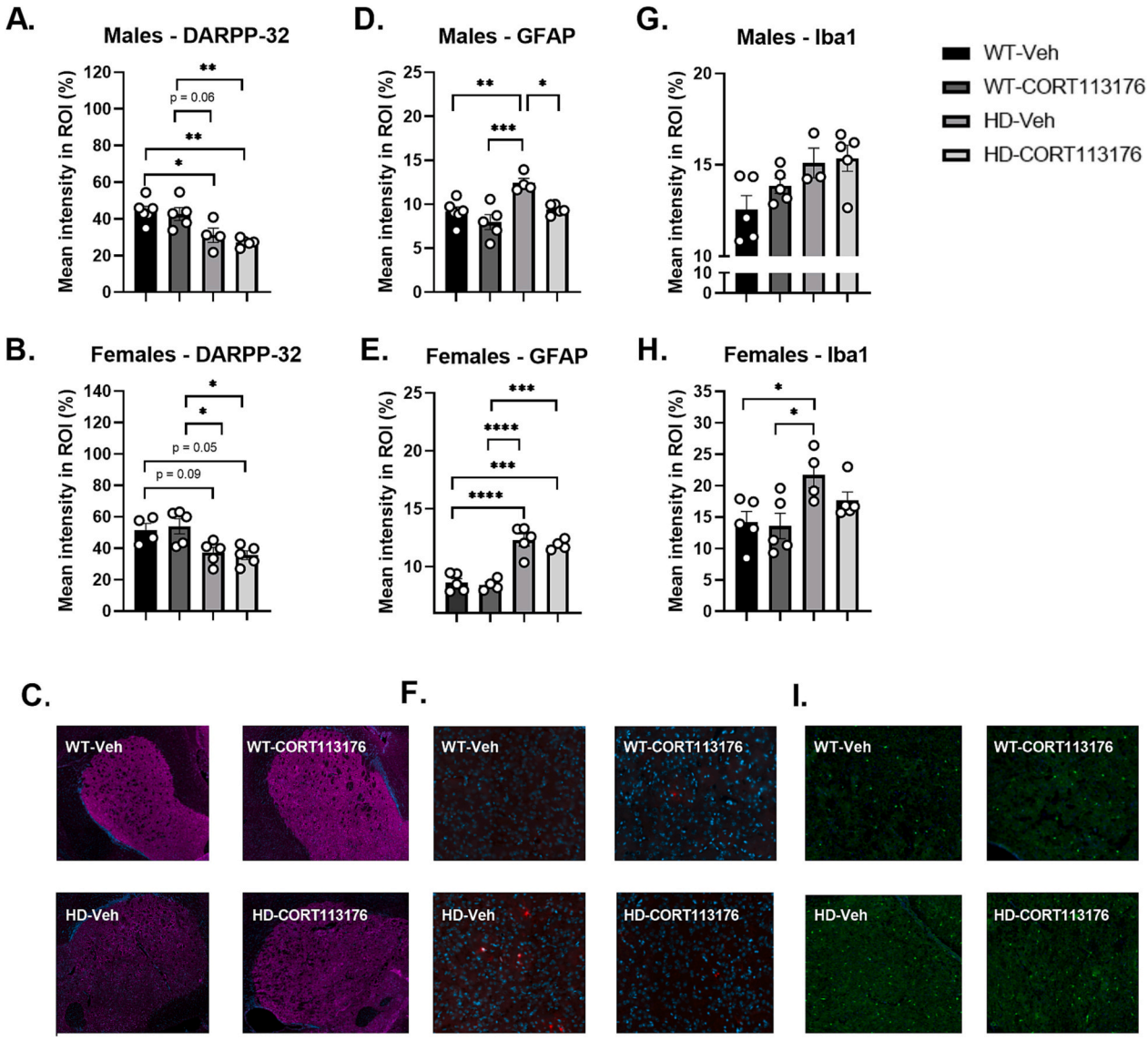

Fig. 4. Immunohistochemistry of markers related to the HD genotype in the dorsolateral striatum of male and female R6/2 mice. (A) The effect of the HD genotype and CORT113176 on DARPP32 intensity in the male dorsolateral striatum and (B) in female dorsolateral striatum. (C) Representative images of the DARPP32 staining in the dorsolateral striatum (purple = DARPP32, blue = DAPI). (D) The effect of the HD genotype and CORT113176 on GFAP intensity in the male dorsolateral striatum and (E) in female dorsolateral striatum. (F) Representative images of the GFAP staining in the dorsolateral striatum (red = GFAP, blue = DAPI). (G) The effect of the HD genotype and CORT113176 on Iba1 intensity in the male dorsolateral striatum and (H) in female dorsolateral striatum. (I) Representative images of the Iba1 staining in the striatum (green = Iba1, blue = DAPI). Data presented as mean + S.E.M. and analysed by two-way ANOVA with Tukey's multiple comparison represented as $^{*}p < 0.05$, $^{**}p < 0.01$, $^{***}p < 0.001$,$^{****}p < 0.0001$. Missing values are due to significant outliers or technical errors. (For interpretation of the references to colour in this figure legend, the reader is referred to the web version of this article.)

(MSNs). In both sexes, we observed a significant reduction of DARPP32 intensity within the dorsolateral striatum in the vehicle-treated HD mice compared to the WT mice (Fig. 4.A, HD: $p = 0.0001$, F(1,16) = 25.01 and 4.B, HD: $p = 0.0007$, F(1,15) = 17.96), and treatment with CORT113176 did not influence this in either male or female mice. Astrocyte and microglia activity was assessed by GFAP and Iba1 staining, respectively. In the dorsolateral striatum, GFAP immunoreactivity was significantly increased in both male and female HD mice compared to WT mice (Fig. 4.D, HD: $p = 0.001$, F(1,16) = 16.09 and 4.E HD: $p < 0.0001$, F (1,14) = 83.92) and treatment with CORT113176 normalized GFAP levels in male, but not in female mice (Fig. 4.D, CORT11316: $p = 0.0027$, F(1,16) = 12.59 and 4.E). A significant genotype effect was observed for Iba1 immunoreactivity in the dorsolateral striatum of both male and female mice (Fig. 4.G, HD: $p = 0.0157$, F(1,14) = 7.588 and 4.H, HD: $p = 0.0056$, F(1,15) = 10.43). However, dorsolateral striatal Iba1 staining was unaffected in both sexes by treatment with CORT113176.

Next, we evaluated astrocyte and microglia markers in the different regions of the hippocampus; CA1, CA3 and dentate gyrus (DG). Within the CA3 region of the males, a significant reduction was observed for GFAP staining (Fig. 5.B) and a trend in the DG between the WT and vehicle-treated HD (Fig. 5.C, $p = 0.06$). Within the CA1, CA3 and DG of the male mice, a significant interaction effect was observed for GFAP (CA1; $p = 0.0335$, F(1,15) = 5.559, CA3; $p = 0.0158$, F(1,15) = 7.543, DG; $p = 0.0276$, F(1,15) = 6.046). Similar to the dorsolateral striatum, CORT113176 treatment tended to normalize this HD effect, although not significantly different compared to either WT or vehicle-treated HD mice in all hippocampal regions (Fig. 5.A, $p = 0.07$, Fig. 5.C, p = 0.07).

In the female hippocampus, a significant genotype effect was observed for GFAP intensity in the CA1 region and the and a trend for the CA3 region, which was unaffected by CORT113176 treatment (Fig. 5.A-C, CA1, HD; $p = 0.0384$, F(1,15) = 5.151, DG, HD; ($p = 0.0479$, F(1,15) = 4.638, CA3, HD; ($p = 0.0505$, F(1,15) = 4.522).

Within the CA1 and CA3 region, a significant interaction effect was found for Iba1 and a trend within the DG (CA1; $p = 0.0124$, F(1,15) = 8.061, CA3; $p = 0.0157$, F(1,16) = 7.298, DG; $p = 0.0768$, F(1,17) = 3.550). Iba1 intensity in the male CA1 region tended to decrease (Fig. 5. G, $p = 0.08$), which was significantly increased in the CA1 and CA3 region with CORT113176-treatment (Fig. 5.G and 5.H).

In the female HD hippocampus, a significant genotype effect was observed in all regions (CA1, HD; $p = 0.0059$, F(1,15) = 0.1418, CA3, HD; $p = 0.0053$, F(1,15) = 10.62, DG, HD; $p = 0.0061$, F(1,15) = 10.16). In vehicle-treated HD mice there was a trend towards an increase of Iba1 intensity as compared to WT in the CA1 and DG (Fig. 5.J, $p = 0.10$) and this was unaffected by CORT113176 treatment (Fig. 5.L, p = 0.10). A similar trend was observed in the CA3 region after CORT113176 treatment (Fig. 5.K., p = 0.10).

3.2. Experiment 2

In our first experiment we observed unanticipated sex differences, which resulted in a loss of statistical power. Therefore, we aimed to replicate and further characterize the potential beneficial effects of CORT113176 treatment in a larger cohort of male R6/2 mice. A gait analysis was included to better assess movement disturbances related to HD. The WT-CORT113176 control group was not included in experiment 2 as we did not observe effects of CORT113176 on any measured parameter (clasping score, grip strength, bodyweight, DARPP-32 expression or glial cell activity) in these mice.

3.2.1. CORT113176 treatment delays several motor function symptoms in male HD mice

In line with our previous experiment, we observed significant time effects for grip strength, clasping score and bodyweight (Supplementary 2.A, 2.B, and 2.C,) and a significant interaction of time with CORT113176 treatment for the grip strength and clasping test (Supplementary 2.A; $p < 0.0001$, F(10,126) = 23.25 and Supplementary 2.B; $p < 0.0001$, F(10, 124) = 27.26). A decline in forelimb grip strength was observed starting from week 1 for both vehicle- and CORT113176-treated HD mice, but treatment with CORT113176 delayed this process, reaching a trend between vehicle- and CORT113176-treated HD groups at week 4 and a significant difference at week 5 (Fig. 6.A, $p = 0.07$ and $p < 0.05$). HD mice again increased clasping score over time, which was delayed in the CORT113176-treated HD mice compared to the vehicle-treated HD mice, reaching a significant difference starting from week 2 until week 5 (Fig. 6.B) HD mice also showed significantly lower bodyweight compared to WT mice starting from week 3, which was unaffected by CORT113176 treatment (Fig. 6.C). Finally, epileptic seizures were documented and occurred mostly in the vehicle-treated HD mice (Fig. 6.D). One epileptic seizure was observed in a CORT113176-treated HD mouse near the end of the study while in vehicle-treated HD mice these seizures were also observed in several mice earlier throughout the study (Fig. 6.E, $p = 0.03$).

The CatWalk gait analysis was performed to evaluate any disturbances in movement related to the HD phenotype. The stride length, defined as the distance between successive placement of the same paw, was increased for the vehicle-treated HD mice compared to the WT mice, reaching a significant difference for several paws and a trend for the combined hind paws at day 15 (Fig. 6.F, RF: $p < 0.05$, RH: $p < 0.05$, FP: $p < 0.05$ and HP: $p = 0.09$). No differences were observed between the WT and CORT113176-treated HD mice on day 15. On day 29, the stride length of vehicle-treated HD mice was significantly decreased compared to the WT and CORT113176 treatment did not influence this (Fig. 6.G).

The support on paw number describes the percentage of time that an animal supports itself during a step cycle on two diagonal, three or four paws. On day 15, a significant increase on support on three paws was observed and a trend towards a decrease in the support on diagonal paws for the vehicle-treated HD mice was observed compared to the WT mice (Fig. 6.H, $p < 0.05$ and $p = 0.07$). No differences were observed between the WT and CORT113176-treated HD mice at day 15. On day 29, HD mice showed a significant increased support on three paws and a significant decreased support on diagonal paws as compared to WT, while CORT113176 treatment did not influence this (Fig. 6.I, $p < 0.001$ and $p < 0.01$).

3.2.2. The R6/2 mouse model exhibit a dysregulated HPA-axis that is unaffected by CORT113176 treatment

Several aspects of the HPA-axis were measured in the HD mice. In accordance with our previous findings, a significant increase of corticosterone was observed in HD mice as compared to WT mice on day 34 (Fig. 7.A, $p < 0.05$ and $p < 0.01$). CORT113176 did not affect the corticosterone levels in HD mice. Larger adrenal glands were also observed in the HD mice with a significantly increase in the CORT113176-treated HD mice compared to WT (Fig. 7.B, $p < 0.05$). In the hypothalamus, a non-significant downregulation of *Crh* was observed in HD mice compared to WT mice, which was not influenced by CORT113176 treatment (Fig. 7.C).

3.2.3. CORT113176 has region-specific effects on glial cells in HD mice

The previously measured biomarkers involved with HD were reassessed to validate our previous findings. In the dorsolateral striatum, a significant increase of GFAP and a trend for Iba1 intensity was observed in the HD mice compared to the WT mice and CORT113176 treatment significantly reduced the GFAP intensity, while the Iba1 intensity was unaffected (Fig. 8.A, $p = 0.0024$ and Fig. 8.B, $p = 0.0189$). A significant decrease in DARPP32 staining intensity was observed in the HD mice, which was significantly increased after CORT113176 treatment (Fig. 8. C, $p < 0.0001$, $p = 0.0424$).

In the hippocampus, decreased GFAP and Iba1 intensity were observed in the CA1 region of the HD mice as compared to the WT mice and both parameters were significantly normalized by CORT113176 treatment (Fig. 8.D and 8.G). CORT113176 treatment increased GFAP and Iba1 intensity compared to vehicle-treated HD mice (Fig. 8.E and 8.

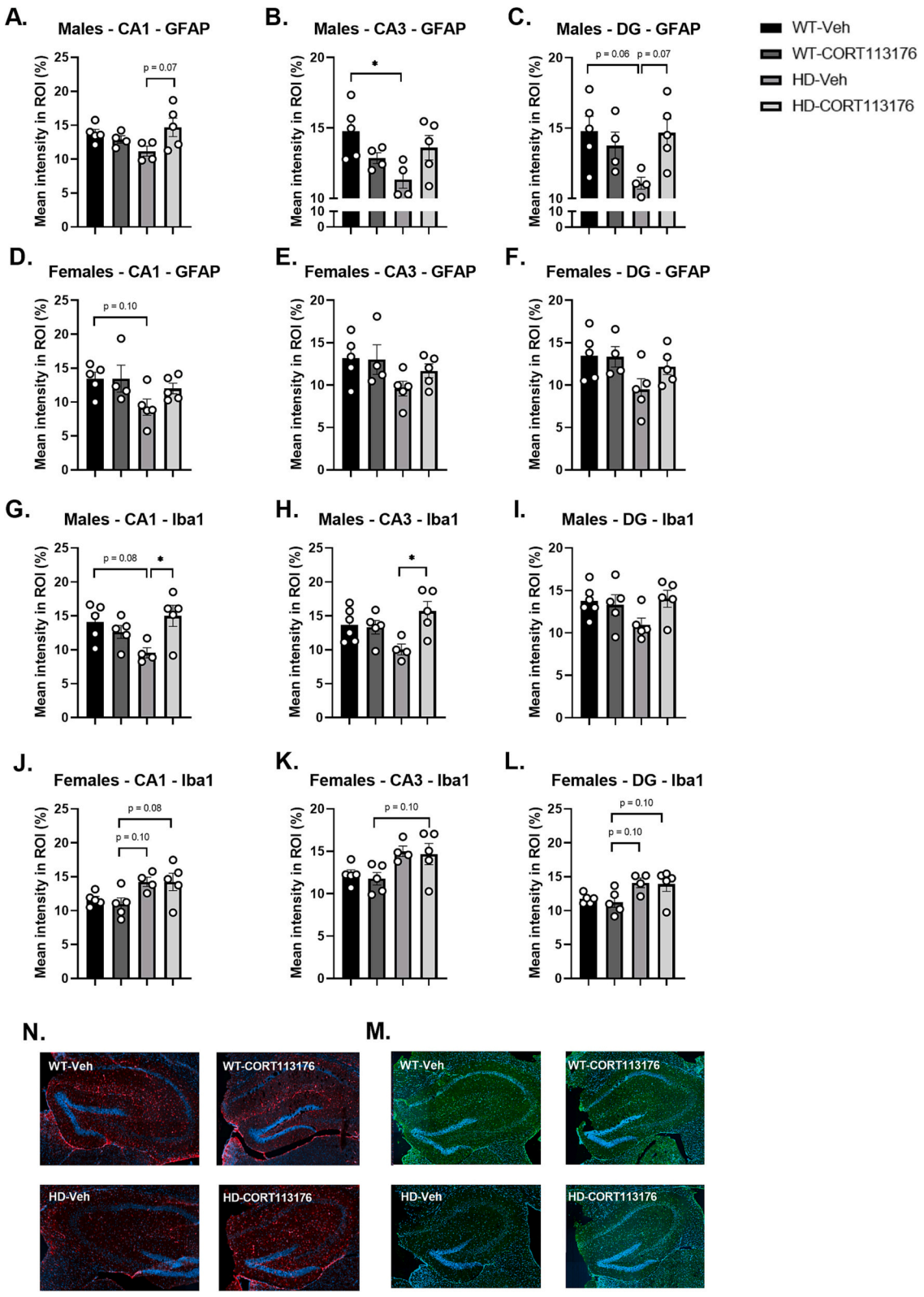

Fig. 5. Immunohistochemistry of markers related to the HD genotype in the CA1, CA3 and DG of the hippocampus of male and female R6/2 mice. The effect of the HD genotype and CORT113176 on GFAP intensity in the (A) CA1, (B) CA3 and (C) DG of the male hippocampus. The effect of the HD genotype and CORT113176 on GFAP intensity in the (D) CA1, (E) CA3 and (F) DG of the female hippocampus. The effect of the HD genotype and CORT113176 on Iba1 intensity in the (G) CA1, (H) CA3 and (I) DG of the male hippocampus. The effect of the HD genotype and CORT113176 on Iba1 intensity in the (J) CA1, (K) CA3 and (L) DG of the female hippocampus. (M) Representative images of the Iba1 staining in the hippocampus (green = Iba1, blue = DAPI). (N) Representative images of the GFAP staining in the hippocampus (red = GFAP, blue = DAPI). (For interpretation of the references to colour in this figure legend, the reader is referred to the web version of this article.)

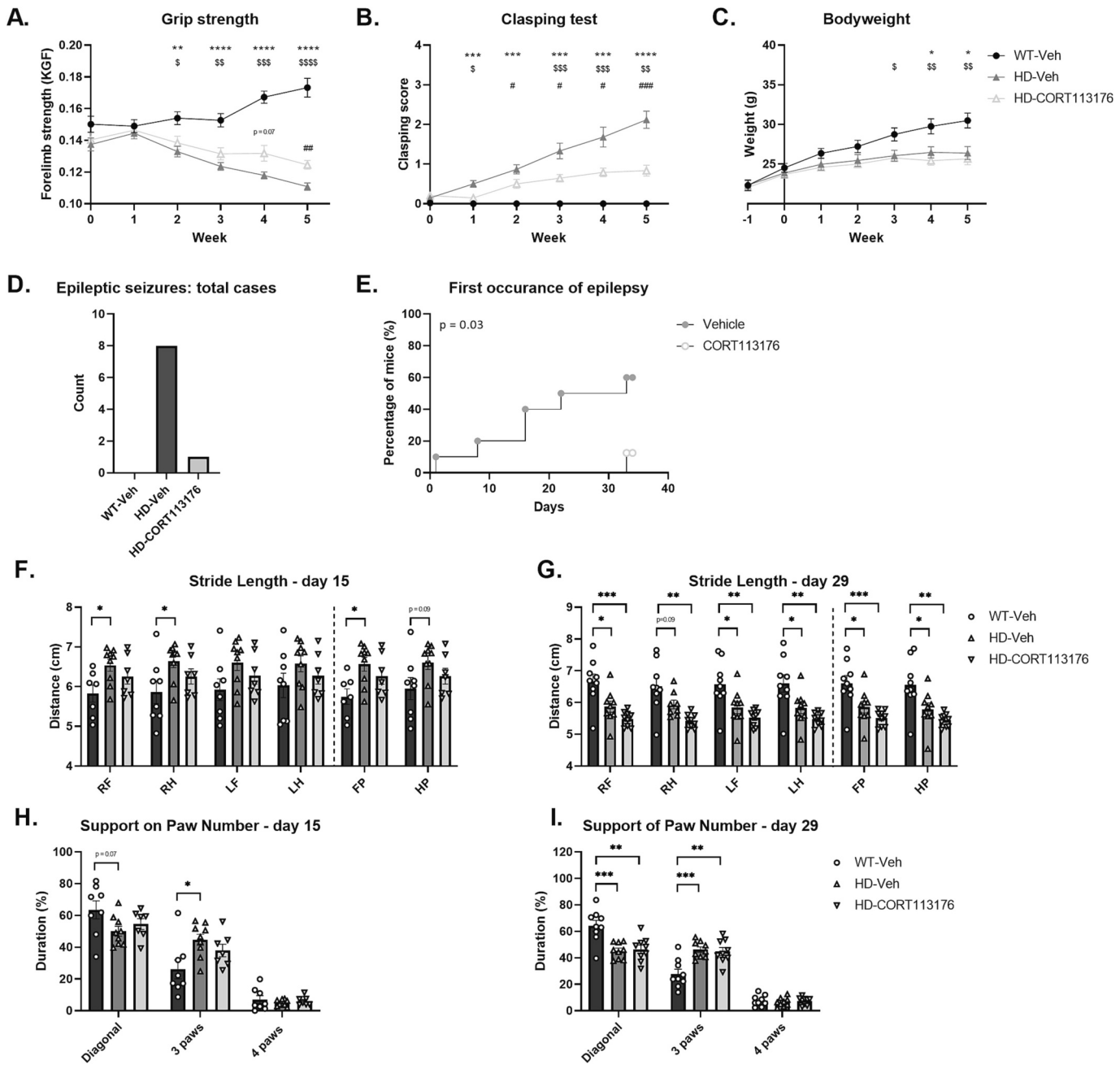

Fig. 6. Functional parameters of the male R6/2 mice (follow-up). (A) The effect of the HD genotype and CORT113176 on forelimb grip strength, (B) hindlimb clasping and (C) body weight over time in male R6/2 mice. (D) Total number of epileptic seizures of male R6/2 mice. (E) Kaplan-Meier analysis for first occurrences of epilepsy. (F) The effect of the HD genotype and CORT113176 on the stride length on day 15 and (G) on day 29 in male R6/2 mice. (H) The effect of the HD genotype and CORT113176 on support on paw number on day 15 and (I) on day 29 in male R6/2 mice. (A-C) Data presented as mean + S.E.M. and analysed by mixed-effects model with repeated measures. Individual timepoints were analysed by two-way ANOVA with Tukey's multiple comparison. (F—I) Other data presented as mean + S.E.M. and analysed by one-way ANOVA with Tukey's multiple comparison represented as * $p < 0.05$, ** $p < 0.01$, *** $p < 0.001$,**** $p < 0.0001$ (* = WT-Veh vs HD-Veh, $ = WT-Veh vs HD-CORT113176 and # = HD-Veh vs HD-CORT113176). Missing values are due to significant outliers or technical errors.

I) while in the DG a decrease in both GFAP and Iba1 was observed (Fig. 8.F and 8.J).

3.2.4. CORT113176 treatment reduces the formation of mutant Huntingtin aggregates in the striatum and in the CA1 region of the hippocampus

The formation of mHtt aggregates was assessed as these are considered the hallmark of the HD phenotype. In the striatum, vehicle-treated HD mice showed a significant increase in the number of aggregates as compared to the WT mice (Fig. 9.A, $p < 0.01$). Treatment with CORT113176 significantly decreased this number of mHtt aggregates (Fig. 9.A, $p < 0.05$.) and the aggregates were of a similar size in vehicle- and CORT113176-treated HD groups (Fig. 7.B).

In the CA1 region of the hippocampus, the total number of aggregates was significantly increased in HD mice compared to WT mice. CORT113176-treated mice had significantly fewer aggregates in this brain region compared to vehicle-treated HD mice (Fig. 9.E, $p < 0.0001$, $p < 0.01$). In addition, the CORT113176-treated mice display smaller aggregates compared to the vehicle-treated HD mice (Fig. 9.F, $p < 0.01$) resulting in a smaller total aggregate area in the CA1 region (Fig. 9.G, $p < 0.01$). In the CA3 region and the dentate gyrus (DG), mHtt aggregates

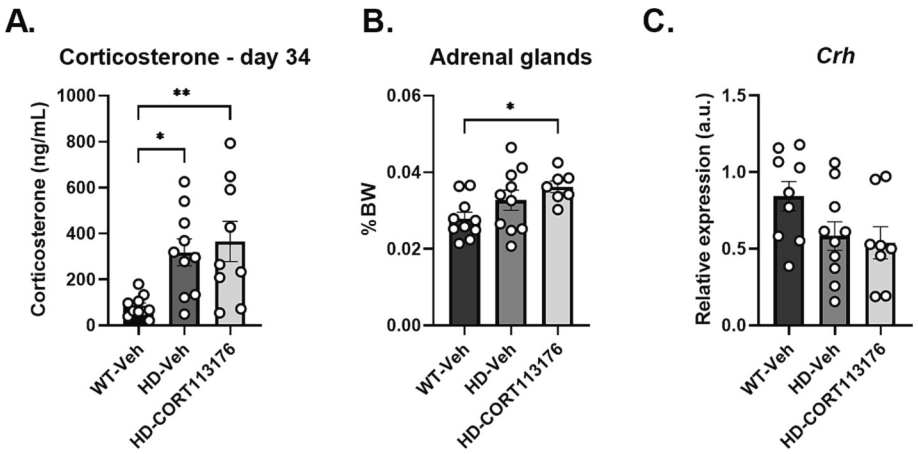

Fig. 7. The effect of the HD genotype and CORT113176 on the HPA-axis in male R6/2 mice. (A) Corticosterone levels at 1 PM on day 34. *(B)* Adrenal weight. *(C) CrH* expression in the hypothalamus. Data presented as mean + S.E.M. and analysed by one-way ANOVA with Tukey's multiple comparison represented as * $p < 0.05$, ** $p < 0.01$, *** $p < 0.001$,**** $p < 0.0001$. Missing values are due to significant outliers or technical errors.

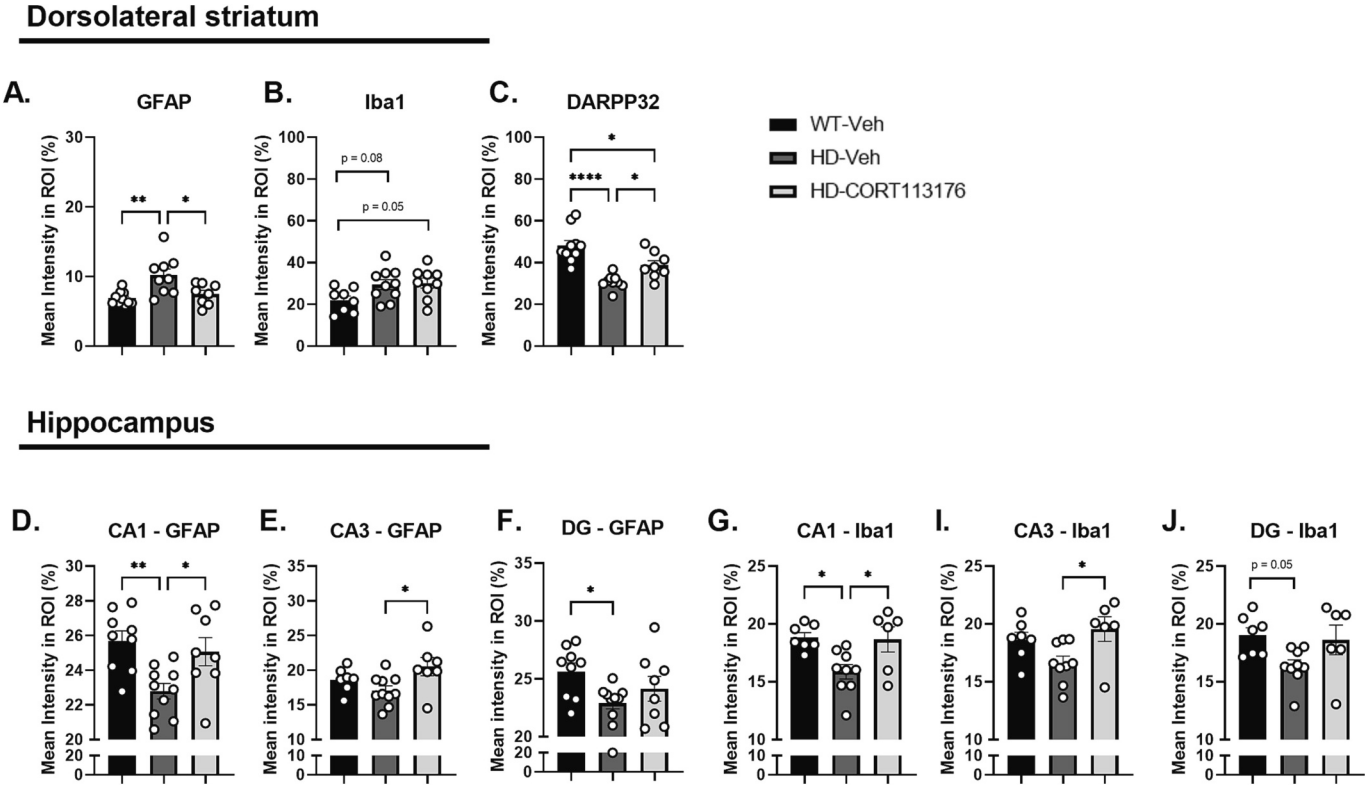

Fig. 8. Immunohistochemistry of markers related to the HD genotype in the dorsolateral striatum and regions of the hippocampus of male R6/2 mice. (A) The effect of the HD genotype and CORT113176 on GFAP intensity and (B) on Iba1 intensity and (C) on DARPP32 intensity in the male dorsolateral striatum. (D) The effect of the HD genotype and CORT113176 on GFAP intensity in the CA1 and (E) CA3 and (F) DG of the male hippocampus. (G) The effect of the HD genotype and CORT113176 on Iba1 intensity in the CA1 and (I) CA3 and (J) DG of the male hippocampus in the male hippocampus. Data presented as mean + S.E.M. and analysed by one-way ANOVA with Tukey's multiple comparison represented as * $p < 0.05$, ** $p < 0.01$, *** $p < 0.001$,**** $p < 0.0001$. Missing values are due to significant outliers or technical errors.

were observed in similar numbers and size regardless of treatment (Fig. 9.I – 7.O), although smaller in both number and size compared to the CA1.

4. Discussion

In this study, we evaluated the efficacy of CORT113176, a selective GR antagonist, to attenuate the symptoms of HD in the R6/2 mouse model. Here, we show in two independent studies that CORT11376 delays several motor and neuropathological symptoms of HD in male mice, and that these beneficial effects are less pronounced or absent in female mice.

In the male mice, we observed that the treatment with CORT113176 alleviated several HD-related symptoms. As such, treatment with CORT113176 partially improved grip strength and significantly reduced clasping score. The strong attenuation of clasping with CORT113176 treatment suggests efficacy in the central nervous system (CNS) as increased clasping reflects degradation of the cortico-striatal pathway.

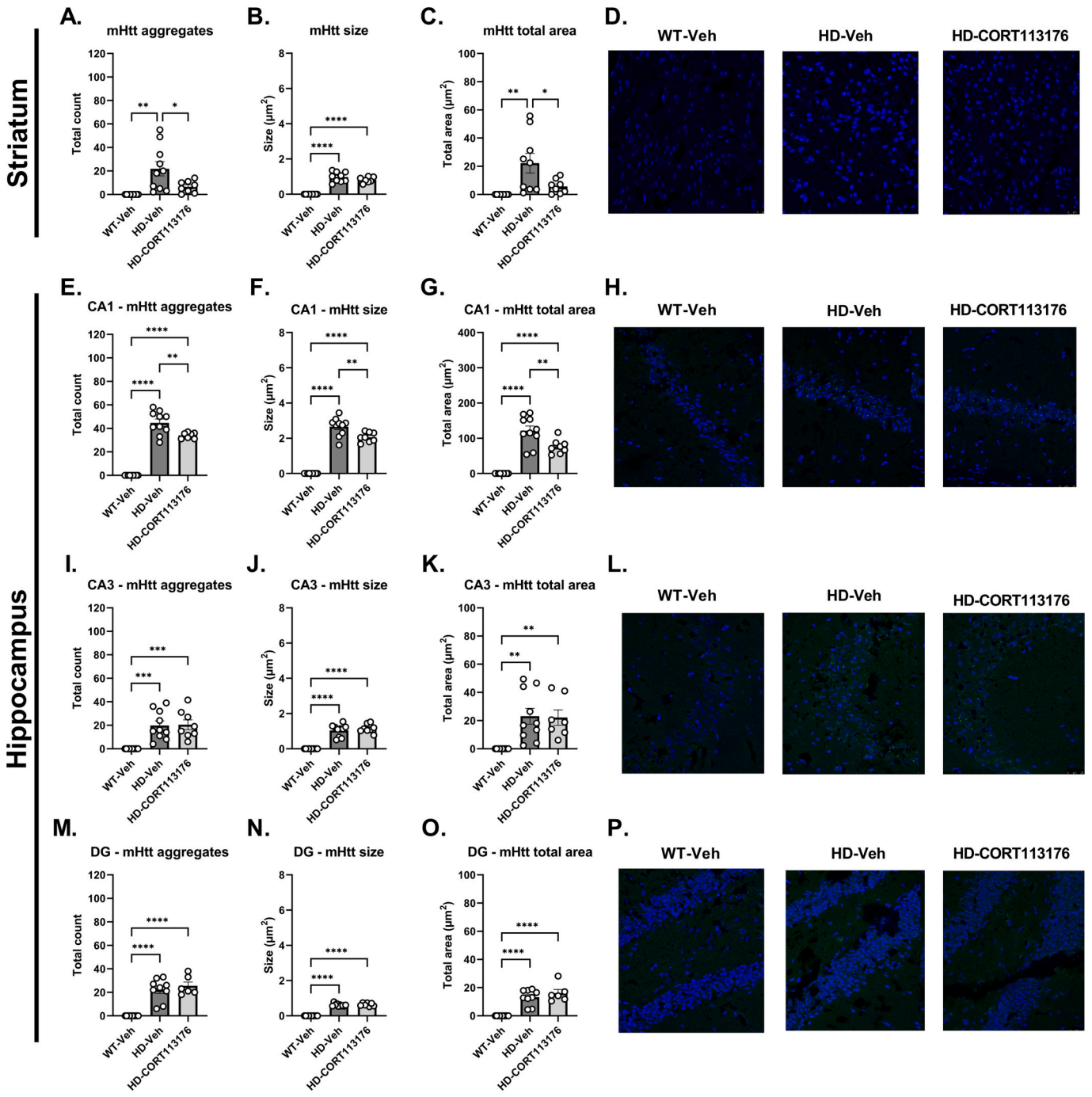

Fig. 9. The effect of the HD genotype and CORT113176 on mHtt aggregates in the striatum and different regions of the hippocampus in male R6/2 mice. (A) Total number of mHtt aggregates, (B) average mHtt aggregate size and (C) total mHtt area within the striatum of male R6/2 mice. (D) Representative images of mHtt aggregates in the striatum (green = mHtt, blue = DAPI). (E) Total number of mHtt aggregates, (F) average mHtt aggregate size and (G) total mHtt area in the CA1 region of the hippocampus of male R6/2 mice. (H) Representatives images of mHtt aggregates in the CA1 region of the hippocampus (green = mHtt, blue = DAPI). (I) Total number of mHtt aggregates, (J) average mHtt aggregate size and (K) total mHtt area in the CA3 region of the hippocampus of male R6/2 mice. (L) Representative images of mHtt aggregates in the CA3 region of the hippocampus (green = mHtt, blue = DAPI). (M) Total number of mHtt aggregates, (N) average mHtt aggregate size and (O) total mHtt area in the DG of the hippocampus of male R6/2 mice. (P) Representative images of mHtt aggregates in the DG of the hippocampus (green = mHtt, blue = DAPI). Data presented as mean + S.E.M. and analysed by one-way ANOVA with Tukey's multiple comparison represented as * $p < 0.05$, ** $p < 0.01$, *** $p < 0.001$,**** $p < 0.0001$. Missing values are due to significant outliers or technical errors. (For interpretation of the references to colour in this figure legend, the reader is referred to the web version of this article.)

Grip strength reflects muscle atrophy (Haber, 2016), but may also mirror neuronal afferents to the muscle, and the mechanisms behind improved muscle function are therefore more difficult to interpret. In the gait analysis, CORT113176 treatment also attenuated the initial increase in stride length, which mimics the hyperkinesia caused by disturbances in the basal ganglia-thalamocortical circuit, that is also observed in patients with HD (Delval et al., 2006; Casaca-Carreira et al., 2015; Park, 2016). Furthermore, in both sexes CORT113176 treatment reduced the occurrence of epileptic seizures, a feature that is also commonly found in JHD (Thakor et al., 2021; Cepeda et al., 2019).

Taken together, there was a clear efficacy of CORT113176 in the CNS, predominantly in male mice.

CORT113176 treatment did delay the loss of DARPP-32 expression in the dorsolateral striatum. This is in accordance with the improvements in motor function associated with the striatum as observed with the clasping test in the cortico-striatal pathway in addition to improved gait. Movement execution by the cortico-striatal pathway is mediated by two different types of MSNs; the excitatory D1R-MSN pathway and inhibitory D2R-MSN pathway (Bergonzoni et al., 2021). Imbalance between these two pathways is thought to be the cause of motor disturbances and the D1R/D2R ratio determines either a hyper- or hypokinetic disorder (Albin et al., 1995). The D2R-MSNs are more susceptible in the early stages of HD resulting in hyperkinesia which causes involuntary movements (Sapp et al., 1995; Albin et al., 1992; Hedreen and Folstein, 1995). The observed reduced clasping score and improved gait after CORT113176 treatment could reflect fewer involuntary movements and therefore less degradation of the D2R-MSNs. Hyperkinesia transitions into hypokinesia by degradation of the D1R-MSNs in the later stages of HD, resulting in akinetic movements (Delval et al., 2006; Casaca-Carreira et al., 2015; Deng et al., 2004; Lanciego et al., 2012). Hypokinesia was also observed in our HD mice in the gait analysis and CORT113176 treatment was unable to prevent this. Altogether, these observations suggest that CORT113176 maintains a proper D1R/D2R balance in the early stages of HD, therefore being more effective in the early stages rather than the later stages. In line with this, epileptic seizures did still occur in the CORT113176-treated HD mice near the end (but not earlier) of the study in both male and female mice, also suggesting CORT113176 is more effective in the earlier stages of HD rather than the later stages.

Glial cells provide support and protection to neurons. Increased activation of glial cells is associated with neuroinflammation and is a common characteristic in neurodegenerative diseases, including HD (Pekny and Nilsson, 2005; Wilton and Stevens, 2020). In accordance with other studies, we observed an upregulation of GFAP in male and female HD mice compared to WT mice, indicating higher astrocyte activity in the striatum (Wilton and Stevens, 2020; Al-Dalahmah et al., 2020; Faideau et al., 2010). In male mice, this may have been driven in part by elevated corticosterone leves (Rozovsky et al., 1995). In contrast, in the hippocampus we observed a reduced density of GFAP-immunoreactive astrocytes in male and female HD mice. These seemingly contradicting results between brain regions reflect the heterogeneity of astrocytes, which exhibit a different transcriptional profile and respond differently to stimuli in both normal and diseased conditions (Al-Dalahmah et al., 2020; Chai et al., 2017). Contrary to our results, a single study showed increased levels of GFAP in the hippocampus in R6/2 mice at 15 weeks of age (Etxeberria-Rekalde et al., 2020). We speculate that in a complex disease state such as HD, it is possible that the individual astrocytes states have an alternative or even opposite response to the different stages of HD progression.

Similar to astrocytes, microglia activation is observed in neurodegenerative diseases as well as after chronic stress (Frank et al., 2007; Sugama, 2009). In the striatum, we observed an increase of Iba1 intensity indicating higher microglia activity in both male and female HD mice compared to WT which was unaffected by CORT113176 treatment. In the hippocampus we observed a sex-specific response of microglia to HD; with a downregulation in male mice and a trend towards upregulation in female mice. Microglia also exhibit heterogeneity across different brain regions with stress being a key mediator of microglia density (Tan et al., 2020). Sex differences have been described for microglia with regards to response to sex hormones and other stimuli, including those involved in neurodegeneration (Vegeto et al., 2020). However, no studies in HD specifically have been performed to delineate possible sexual dimorphism in microglia response, and so this is difficult to interpret. Also, while we observed an effect of CORT113176 on Iba1+ microglia in the hippocampus, we did not observe an effect on Iba1+ microglia in the striatum. This lack of effect could be explained by different phenotypes of microglia, but we do not have this information in our study. Nonetheless, Iba1 is a microglia activity marker and therefore a relevant readout for neuroinflammation in HD. Our data suggest that the regulation of glial cells is GR dependent as the different response to HD progression in the brain regions could be prevented by GR antagonism and this most likely contributes to the delayed symptoms of HD.

The presence of mHtt aggregates in the brain is the most distinguishing neuropathological characteristic for HD. CORT113176 treatment significantly reduced the number of mHtt aggregates in the striatum and this reduction could also explain the delayed loss of DARPP-32 expression. Nonetheless, mHtt aggregates are not the sole cause of neurodegeneration, and other mechanisms caused by the toxic gain of function of mHtt, including excitotoxicity and impaired glutamate uptake, also contribute to neuronal death within this brain region (Gil and Rego, 2008; Cicchetti et al., 2011; Lievens et al., 2001). CORT113176 treatment also reduced the total number and size of the mHtt aggregates in CA1 region of the hippocampus. Cognitive deficits are observed earlier (4–8 weeks of age) compared to motor deficits (8–10 weeks of age) in the R6/2 model (Carter et al., 1999; Puigdellivol et al., 2016). Also in patients with HD, early hippocampal impairment defines the onset of HD before other more characteristic symptoms of HD appear (Begeti et al., 2016; Paulsen, 2010; Beglinger et al., 2010). This highlights the importance of studying multiple brain regions in the development of HD, even though the striatum is regarded as the most vulnerable to mHtt and neurodegeneration. The aggregates in the CA1 region can be observed as early as week 3, several weeks before this is observed in other brain regions, such as in the DG (7 weeks) or the striatum (10 weeks) (Murphy et al., 2000). We also observed a higher aggregate load within the CA1 compared to the other hippocampal subregions. These aggregates in the CA1 were found to be associated with a reduction of long-term potentiation (LTP) and synaptic long-term depression (LTD). This in turn can lead to learning impairments which are observed in week 5 in the R6/2 model (Murphy et al., 2000; Lione et al., 1999). It is currently unclear if CORT113176 treatment improves cognitive function in R6/2 mice since this has not been evaluated.

Elevated levels of glucocorticoids are found in both patients with HD and HD mouse models (Aziz et al., 2009; Bjorkqvist et al., 2006). We observed an increase of corticosterone levels in male R6/2 mice, but not in female mice. This difference could explain the much weaker effect of CORT113176 on HD progression in female mice, as here HD progression may depend less on increased GR signaling compared to the male mice. It seems that the HD phenotype develops differently between male and female mice as shown by the differences in bodyweight gain, response of glial cells and the absence of increased levels of corticosterone in the female HD mice. In humans, other than a slightly faster progression in female patients, no major differences between sexes in the development of HD are known, as both male and female patients exhibit increased levels of cortisol (Aziz et al., 2009; Zielonka et al., 2013; Zielonka and Stawinska-Witoszynska, 2020). The lack of increased corticosterone levels in female subjects might be related to the R6/2 model rather than the actual disease development in humans. Sex differences in HD progression and effects of CORT113176 may relate to circulating sex steroids, but we lack information on this from our study.

Increased corticosterone in neurodegenerative disease are in line with the classical ‘cascade’ hypothesis, where a vicious cycle is suggested between HPA-axis overactivation and neurodegeneration (Herbert et al., 2006). The evidence for the involvement of the GR in the development of neurodegeneration is growing. Higher levels of cortisol are found in patients with Alzheimer's Disease, Parkinson's Disease, ALS and HD, and this can contribute to the development of these disorders (Aziz et al., 2009; Vyas et al., 2016; Sharma and Singh, 2020; Kibel and Drenjancevic-Peric, 2008; De Nicola et al., 2020). Although the exact mechanisms are still unknown, the fact that GR is involved in multiple neurodegenerative disorders suggests a possible general mechanism in neurodegenerative disorders. The observation that treatment with CORT113176 is effective in different models for neurodegeneration

supports this notion (Pineau et al., 2016; Meyer et al., 2020).

In conclusion, we show that several symptoms of HD can be attenuated in male R6/2 mice by treatment with CORT113176. CORT113176 treatment delayed loss of DARPP-32 expression and motor function impairment, and reduced formation of mHtt aggregates in the striatum and hippocampus. The fact that CORT113176 is effective in a variety of neurodegenerative disorders, including Alzheimer's Disease, ALS and HD, supports the notion of a general GR-mediated mechanism in neurodegenerative diseases. CORT113176 seems to be more effective in the early rather than the later stages of HD progression and unraveling the changes throughout HD progression and specifically how this influences the efficacy of CORT113176 is of great importance in understanding the role of GR in neurodegeneration.

Supplementary data to this article can be found online at https://doi.org/10.1016/j.expneurol.2024.114675.

Funding

Onno Meijer received funding from Corcept Therapeutics for the research in this manuscript.

Author' contributions

MG: design of work, acquisition, analysis, interpretation of data, drafted and revised manuscript
FL: acquisition, analysis, interpretation of data
XB: acquisition, analysis, interpretation of data
AM: acquisition, analysis, interpretation of data
HH: design of work, interpretation of data, revised manuscript
JK: interpretation of data, revised manuscript
WC: design of work, interpretation of data, revised manuscript
OC: design of work, interpretation of data, revised manuscript
All authors have approved the manuscript and agree with the submission.

CRediT authorship contribution statement

Max Gentenaar: Conceptualization, Data curation, Formal analysis, Investigation, Methodology, Visualization, Writing – original draft, Writing – review & editing. **Fleur L. Meulmeester:** Data curation, Formal analysis. **Ximaine R. van der Burg:** Data curation, Formal analysis. **Anna T. Hoekstra:** Data curation, Formal analysis. **Hazel Hunt:** Conceptualization, Funding acquisition, Project administration, Resources, Writing – original draft. **Jan Kroon:** Formal analysis, Supervision, Writing – original draft, Writing – review & editing. **Willeke M.C. van Roon-Mom:** Conceptualization, Methodology, Resources, Supervision, Writing – original draft. **Onno C. Meijer:** Conceptualization, Funding acquisition, Supervision, Writing – original draft, Writing – review & editing.

Declaration of competing interest

Hazel Hunt is an employee and Jan Kroon is seconded at Corcept Therapeutics, the pharmaceutical company that designs and develops CORT113176.

The authors declare that they have no known competing financial interests or personal relationships that could have appeared to influence the work reported in this paper.

Data availability

Data will be made available on request.

Acknowledgements

We thank Trea Streefland, Hetty Sips, Amanda Pronk and Salwa Afkir for their excellent technical assistance. We also thank Suzanne de Bot for her clinical insight and expertise.

References

Aartsma-Rus, A., van Putten, M., 2014. Assessing functional performance in the mdx mouse model. J. Vis. Exp. 85.
Albin, R.L., Reiner, A., Anderson, K.D., LSt, Dure, Handelin, B., Balfour, R., et al., 1992. Preferential loss of striato-external pallidal projection neurons in presymptomatic Huntington's disease. Ann. Neurol. 31 (4), 425–430.
Albin, R.L., Young, A.B., Penney, J.B., 1995. The functional anatomy of disorders of the basal ganglia. Trends Neurosci. 18 (2), 63–64.
Al-Dalahmah, O., Sosunov, A.A., Shaik, A., Ofori, K., Liu, Y., Vonsattel, J.P., et al., 2020. Single-nucleus RNA-seq identifies Huntington disease astrocyte states. Acta Neuropathol. Commun. 8 (1), 19.
Aziz, N.A., Pijl, H., Frolich, M., van der Graaf, A.W., Roelfsema, F., Roos, R.A., 2009. Increased hypothalamic-pituitary-adrenal axis activity in Huntington's disease. J. Clin. Endocrinol. Metab. 94 (4), 1223–1228.
Baglietto-Vargas, D., Medeiros, R., Martinez-Coria, H., LaFerla, F.M., Green, K.N., 2013. Mifepristone alters amyloid precursor protein processing to preclude amyloid beta and also reduces tau pathology. Biol. Psychiatry 74 (5), 357–366.
Bartlett, D.M., Cruickshank, T.M., Hannan, A.J., Eastwood, P.R., Lazar, A.S., Ziman, M. R., 2016. Neuroendocrine and neurotrophic signaling in Huntington's disease: implications for pathogenic mechanisms and treatment strategies. Neurosci. Biobehav. Rev. 71, 444–454.
Bates, G.P., Dorsey, R., Gusella, J.F., Hayden, M.R., Kay, C., Leavitt, B.R., et al., 2015. Huntington disease. Nat. Rev. Dis. Primers. 1, 15005.
Begeti, F., Schwab, L.C., Mason, S.L., Barker, R.A., 2016. Hippocampal dysfunction defines disease onset in Huntington's disease. J. Neurol. Neurosurg. Psychiatry 87 (9), 975–981.
Beglinger, L.J., O'Rourke, J.J., Wang, C., Langbehn, D.R., Duff, K., Paulsen, J.S., et al., 2010. Earliest functional declines in Huntington disease. Psychiatry Res. 178 (2), 414–418.
Bergonzoni, G., Doring, J., Biagioli, M., 2021. D1R- and D2R-medium-sized spiny neurons diversity: insights into striatal vulnerability to Huntington's disease mutation. Front. Cell. Neurosci. 15, 628010.
Bjorkqvist, M., Petersen, A., Bacos, K., Isaacs, J., Norlen, P., Gil, J., et al., 2006. Progressive alterations in the hypothalamic-pituitary-adrenal axis in the R6/2 transgenic mouse model of Huntington's disease. Hum. Mol. Genet. 15 (10), 1713–1721.
Carter, R.J., Lione, L.A., Humby, T., Mangiarini, L., Mahal, A., Bates, G.P., et al., 1999. Characterization of progressive motor deficits in mice transgenic for the human Huntington's disease mutation. J. Neurosci. 19 (8), 3248–3257.
Casaca-Carreira, J., Temel, Y., van Zelst, M., Jahanshahi, A., 2015. Coexistence of gait disturbances and chorea in experimental Huntington's disease. Behav. Neurol. 2015, 970204.
Cepeda, C., Oikonomou, K.D., Cummings, D., Barry, J., Yazon, V.W., Chen, D.T., et al., 2019. Developmental origins of cortical hyperexcitability in Huntington's disease: review and new observations. J. Neurosci. Res. 97 (12), 1624–1635.
Chai, H., Diaz-Castro, B., Shigetomi, E., Monte, E., Octeau, J.C., Yu, X., et al., 2017. Neural circuit-specialized astrocytes: transcriptomic, proteomic, morphological, and functional evidence. Neuron. 95 (3), 531–49 e9.
Cicchetti, F., Soulet, D., Freeman, T.B., 2011. Neuronal degeneration in striatal transplants and Huntington's disease: potential mechanisms and clinical implications. Brain. 134 (Pt 3), 641–652.
De Nicola, A.F., Meyer, M., Guennoun, R., Schumacher, M., Hunt, H., Belanoff, J., et al., 2020. Insights into the therapeutic potential of glucocorticoid receptor modulators for neurodegenerative diseases. Int. J. Mol. Sci. 21 (6).
Delval, A., Krystkowiak, P., Blatt, J.L., Labyt, E., Dujardin, K., Destee, A., et al., 2006. Role of hypokinesia and bradykinesia in gait disturbances in Huntington's disease: a biomechanical study. J. Neurol. 253 (1), 73–80.
Deng, Y.P., Albin, R.L., Penney, J.B., Young, A.B., Anderson, K.D., Reiner, A., 2004. Differential loss of striatal projection systems in Huntington's disease: a quantitative immunohistochemical study. J. Chem. Neuroanat. 27 (3), 143–164.
Dufour, B.D., McBride, J.L., 2016. Corticosterone dysregulation exacerbates disease progression in the R6/2 transgenic mouse model of Huntington's disease. Exp. Neurol. 283 (Pt A), 308–317.
Dufour, B.D., McBride, J.L., 2019. Normalizing glucocorticoid levels attenuates metabolic and neuropathological symptoms in the R6/2 mouse model of huntington's disease. Neurobiol. Dis. 121, 214–229.
van Duijn, E., Selis, M.A., Giltay, E.J., Zitman, F.G., Roos, R.A., van Pelt, H., et al., 2010. Hypothalamic-pituitary-adrenal axis functioning in Huntington's disease mutation carriers compared with mutation-negative first-degree controls. Brain Res. Bull. 83 (5), 232–237.
Etxeberria-Rekalde, E., Alzola-Aldamizetxebarria, S., Flunkert, S., Hable, I., Daurer, M., Neddens, J., et al., 2020. Quantification of Huntington's disease related markers in the R6/2 mouse model. Front. Mol. Neurosci. 13, 617229.
Faideau, M., Kim, J., Cormier, K., Gilmore, R., Welch, M., Auregan, G., et al., 2010. In vivo expression of polyglutamine-expanded huntingtin by mouse striatal astrocytes impairs glutamate transport: a correlation with Huntington's disease subjects. Hum. Mol. Genet. 19 (15), 3053–3067.
Frank, M.G., Baratta, M.V., Sprunger, D.B., Watkins, L.R., Maier, S.F., 2007. Microglia serve as a neuroimmune substrate for stress-induced potentiation of CNS pro-inflammatory cytokine responses. Brain Behav. Immun. 21 (1), 47–59.

Gaillard, R.C., Riondel, A., Muller, A.F., Herrmann, W., Baulieu, E.E., 1984. RU 486: a steroid with antiglucocorticosteroid activity that only disinhibits the human pituitary-adrenal system at a specific time of day. Proc. Natl. Acad. Sci. U. S. A. 81 (12), 3879–3882.
Gil, J.M., Rego, A.C., 2008. Mechanisms of neurodegeneration in Huntington's disease. Eur. J. Neurosci. 27 (11), 2803–2820.
Guyenet, S.J., Furrer, S.A., Damian, V.M., Baughan, T.D., La Spada, A.R., Garden, G.A., 2010. A simple composite phenotype scoring system for evaluating mouse models of cerebellar ataxia. J. Vis. Exp. 39.
Haber, S.N., 2016. Corticostriatal circuitry. Dialogues Clin. Neurosci. 18 (1), 7–21.
Hedreen, J.C., Folstein, S.E., 1995. Early loss of neostriatal striosome neurons in Huntington's disease. J. Neuropathol. Exp. Neurol. 54 (1), 105–120.
Herbert, J., Goodyer, I.M., Grossman, A.B., Hastings, M.H., de Kloet, E.R., Lightman, S.L., et al., 2006. Do corticosteroids damage the brain? J. Neuroendocrinol. 18 (6), 393–411.
Hunt, H.J., Belanoff, J.K., Golding, E., Gourdet, B., Phillips, T., Swift, D., et al., 2015. 1H-Pyrazolo[3,4-g]hexahydro-isoquinolines as potent GR antagonists with reduced hERG inhibition and an improved pharmacokinetic profile. Bioorg. Med. Chem. Lett. 25 (24), 5720–5725.
Kibel, A., Drenjancevic-Peric, I., 2008. Impact of glucocorticoids and chronic stress on progression of Parkinson's disease. Med. Hypotheses 71 (6), 952–956.
Kirkwood, S.C., Su, J.L., Conneally, P., Foroud, T., 2001. Progression of symptoms in the early and middle stages of Huntington disease. Arch. Neurol. 58 (2), 273–278.
Lanciego, J.L., Luquin, N., Obeso, J.A., 2012. Functional neuroanatomy of the basal ganglia. Cold Spring Harb. Perspect. Med. 2 (12), a009621.
Lesuis, S.L., Weggen, S., Baches, S., Lucassen, P.J., Krugers, H.J., 2018. Targeting glucocorticoid receptors prevents the effects of early life stress on amyloid pathology and cognitive performance in APP/PS1 mice. Transl. Psychiatry 8 (1), 53.
Lievens, J.C., Woodman, B., Mahal, A., Spasic-Boscovic, O., Samuel, D., Kerkerian-Le Goff, L., et al., 2001. Impaired glutamate uptake in the R6 Huntington's disease transgenic mice. Neurobiol. Dis. 8 (5), 807–821.
Lione, L.A., Carter, R.J., Hunt, M.J., Bates, G.P., Morton, A.J., Dunnett, S.B., 1999. Selective discrimination learning impairments in mice expressing the human Huntington's disease mutation. J. Neurosci. 19 (23), 10428–10437.
Meyer, M., Lara, A., Hunt, H., Belanoff, J., de Kloet, E.R., Gonzalez Deniselle, M.C., et al., 2018. The selective glucocorticoid receptor modulator Cort 113176 reduces neurodegeneration and Neuroinflammation in wobbler mice spinal cord. Neuroscience. 384, 384–396.
Meyer, M., Kruse, M.S., Garay, L., Lima, A., Roig, P., Hunt, H., et al., 2020. Long-term effects of the glucocorticoid receptor modulator CORT113176 in murine motoneuron degeneration. Brain Res. 1727.
Mo, C., Renoir, T., Pang, T.Y., Hannan, A.J., 2013. Short-term memory acquisition in female Huntington's disease mice is vulnerable to acute stress. Behav. Brain Res. 253, 318–322.
Mo, C., Renoir, T., Hannan, A.J., 2014. Effects of chronic stress on the onset and progression of Huntington's disease in transgenic mice. Neurobiol. Dis. 71, 81–94.
Morton, A.J., Lagan, M.A., Skepper, J.N., Dunnett, S.B., 2000. Progressive formation of inclusions in the striatum and hippocampus of mice transgenic for the human Huntington's disease mutation. J. Neurocytol. 29 (9), 679–702.
Murphy, K.P., Carter, R.J., Lione, L.A., Mangiarini, L., Mahal, A., Bates, G.P., et al., 2000. Abnormal synaptic plasticity and impaired spatial cognition in mice transgenic for exon 1 of the human Huntington's disease mutation. J. Neurosci. 20 (13), 5115–5123.
Park, J., 2016. Movement disorders following cerebrovascular lesion in the basal ganglia circuit. J. Mov. Disord. 9 (2), 71–79.
Paulsen, J.S., 2010. Early detection of Huntington disease. Future Neurol. 5 (1).
Pekny, M., Nilsson, M., 2005. Astrocyte activation and reactive gliosis. Glia. 50 (4), 427–434.
Pineau, F., Canet, G., Desrumaux, C., Hunt, H., Chevallier, N., Ollivier, M., et al., 2016. New selective glucocorticoid receptor modulators reverse amyloid-beta peptide-induced hippocampus toxicity. Neurobiol. Aging 45, 109–122.
Puigdellivol, M., Saavedra, A., Perez-Navarro, E., 2016. Cognitive dysfunction in Huntington's disease: mechanisms and therapeutic strategies beyond BDNF. Brain Pathol. 26 (6), 752–771.
Rozovsky, I., Laping, N.J., Krohn, K., Teter, B., O'Callaghan, J.P., Finch, C.E., 1995. Transcriptional regulation of glial fibrillary acidic protein by corticosterone in rat astrocytes in vitro is influenced by the duration of time in culture and by astrocyte-neuron interactions. Endocrinology. 136 (5), 2066–2073.
Sapp, E., Ge, P., Aizawa, H., Bird, E., Penney, J., Young, A.B., et al., 1995. Evidence for a preferential loss of enkephalin immunoreactivity in the external globus pallidus in low grade Huntington's disease using high resolution image analysis. Neuroscience. 64 (2), 397–404.
Schakman, O., Kalista, S., Barbe, C., Loumaye, A., Thissen, J.P., 2013. Glucocorticoid-induced skeletal muscle atrophy. Int. J. Biochem. Cell Biol. 45 (10), 2163–2172.
Sharma, V.K., Singh, T.G., 2020. Navigating Alzheimer's disease via chronic stress: the role of glucocorticoids. Curr. Drug Targets 21 (5), 433–444.
Story, D., Gallien, J., Al-Gharaibeh, A., Sandstrom, M., Rossignol, J., Dunbar, G.L., 2021. Housing R6/2 mice with wild-type littermates increases lifespan. J. Huntingtons. Dis. 10 (4), 455–458.
Sugama, S., 2009. Stress-induced microglial activation may facilitate the progression of neurodegenerative disorders. Med. Hypotheses 73 (6), 1031–1034.
Tan, Y.L., Yuan, Y., Tian, L., 2020. Microglial regional heterogeneity and its role in the brain. Mol. Psychiatry 25 (2), 351–367.
Thakor, B., Jagtap, S.A., Joshi, A., 2021. Juvenile Huntington's disease masquerading as progressive myoclonus epilepsy. Epilepsy Behav. Rep. 16, 100470.
Van Erum, J., Van Dam, D., De Deyn, P.P., 2019. PTZ-induced seizures in mice require a revised Racine scale. Epilepsy Behav. 95, 51–55.
Vegeto, E., Villa, A., Della Torre, S., Crippa, V., Rusmini, P., Cristofani, R., et al., 2020. The role of sex and sex hormones in neurodegenerative diseases. Endocr. Rev. 41 (2), 273–319.
Vegiopoulos, A., Herzig, S., 2007. Glucocorticoids, metabolism and metabolic diseases. Mol. Cell. Endocrinol. 275 (1–2), 43–61.
Vonsattel, J.P., DiFiglia, M., 1998. Huntington disease. J. Neuropathol. Exp. Neurol. 57 (5), 369–384.
Vyas, S., Rodrigues, A.J., Silva, J.M., Tronche, F., Almeida OF, Sousa, N., et al., 2016. Chronic stress and glucocorticoids: from neuronal plasticity to neurodegeneration. Neural Plast. 2016, 6391686.
Wilton, D.K., Stevens, B., 2020. The contribution of glial cells to Huntington's disease pathogenesis. Neurobiol. Dis. 143, 104963.
Zielonka, D., Stawinska-Witoszynska, B., 2020. Gender differences in non-sex linked disorders: insights from Huntington's disease. Front. Neurol. 11, 571.
Zielonka, D., Marinus, J., Roos, R.A., De Michele, G., Di Donato, S., Putter, H., et al., 2013. The influence of gender on phenotype and disease progression in patients with Huntington's disease. Parkinsonism Relat. Disord. 19 (2), 192–197.